Applied Surface Science 278 (2013) 47–51

Contents lists available at SciVerse ScienceDirect

Applied Surface Science

journal homepage: www.elsevier.com/locate/apsusc

# Oxidation of laser-induced plasma species in different background conditions

Matthias Bator, Christof W. Schneider, Thomas Lippert*, Alexander Wokaun

*Paul Scherrer Institute, Department General Energy, Villigen PSI, Switzerland*

ARTICLE INFO

*Article history:*
Available online 26 January 2013

*Keywords:*
Pulsed laser deposition
Rare-earth manganates
Plasma imaging
Plasma characterization
Plasma mass spectrometry

ABSTRACT

The evolution of Lu and LuO species in a laser ablation plasma from different targets has been investigated by simultaneously performing mass spectrometry and plasma imaging. Ablation was achieved with a 248 nm KrF laser from a Lu, a $Lu_2O_5$ and a $LuMnO_3$ target under different background gas conditions. Mass spectrometry measurements show very similar intensities and ratios for the respective species for all three targets under the same ablation conditions. This indicates only a small influence of the target on the final Lu and LuO contents in the plasma, with the major influence coming from collisions with the background gas. Furthermore, spatially, timely and spectrally resolved plasma imaging was utilized to clearly identify the shockwave at the plasma front as the main region for Lu oxidation. A strong decrease of Lu intensities together with a directly correlated increase of LuO was observed toward the outer regions of the plasma.



## 1. Introduction

In recent years the search for materials with novel properties has intensified as the development in particular for applications is pushing to new frontiers. Very promising properties have been found in strongly correlated electron systems [1] such as in strained thin films, thin film interfaces or grain boundaries [2]. Oxides play a major role in this development as various properties, such as highly conducting interface between two insulating layers [3,4], tailor-made charge distributions [5], induced magnetism [6] or multiferroicity [7] could be realized.

For multiferroics, systems with two or more ferroic properties – ferroelectricity, ferromagnetism, ferroelasticity – [8] in the same phase, orthorhombic rare-earth manganates (in our case $LuMnO_3$) are a promising material group. They offer a strong direct coupling between ferroelectricity and antiferromagnetism [9,10] as well as possibly ferromagnetism [11]. For high quality thin film growth, pulsed laser deposition has proven to be one of the most suitable techniques, allowing the usage of multi-elemental targets with predefined composition. Still, the final films often grow oxygen-deficient in vacuum [12]. To counteract this issue, oxidizing background gases such as $O_2$ or $N_2O$ are utilized. Depending on the used target this can be more or less beneficial and therefore, it is important to understand which of the created plasma species are mainly responsible for the oxygen transport into the thin film. To gain a better understanding of the plasma evolution during the ablation process, we investigate the oxidation behavior of Lu in laser induced plasmas from a Lu, a $Lu_2O_3$ and a $LuMnO_3$ target by plasma mass spectrometry and plasma imaging.

## 2. Materials and methods

To investigate the properties of laser induced Lu plasma species, three different Lu-containing targets were investigated: a metal Lu disc target, a ceramic $Lu_2O_3$ disc target, and a cylindrical ceramic target of hexagonal-$LuMnO_3$. For the ablation of these targets, a KrF excimer laser ($\lambda$ = 248 nm) was used at a repetition rate of 8 Hz with a laser fluence of ~3.5 J/cm$^2$. A 9 mm × 9 mm mask was imaged onto the target resulting in an approx. 1.7 mm$^2$ spot size. The angle of incidence is 45° for the two disc targets, while the finite area of the laser spot results in a slightly wider range of incidence angles in the case of cylindrical targets (ca. 40–50°). The background pressure was varied from vacuum ($1 \times 10^{-8}$ mbar) to $1.5 \times 10^{-3}$ and $5 \times 10^{-2}$ mbar using $N_2O$ and $O_2$ background gases. The setup is described in more detail in [13].

Plasma mass analysis was performed using a Hiden Analytical EQP/EQS Analyzer and quadrupole mass spectrometer. The system includes an internal ionizer for the measurement of neutral species. Plasma imaging was performed using an Andor Solis USB iStar camera equipped with an acousto-optical tunable filter (AOTF, Brimrose VA210-.40-.65-H) for the range of 400–650 nm. The resolution is ~0.8 nm for the short wavelengths, up to 2.1 nm on the upper end of the range. The settings for gating, frame repetition and delay times are mentioned in the respective parts of the discussion. To image the entire plasma (4 cm) including the target and the mass spectrometer nozzle onto the CCD a Nikkor 28–300 mm lens was used at a distance of 550 mm to the plasma set to a ~200 mm focal length. The mass spectrometry and the plasma imaging were both

* Corresponding author. Tel.: +41 56 310 4076.
*E-mail address:* thomas.lippert@psi.ch (T. Lippert).

0169-4332/$ – see front matter © 2013 Elsevier B.V. All rights reserved.
http://dx.doi.org/10.1016/j.apsusc.2013.01.128

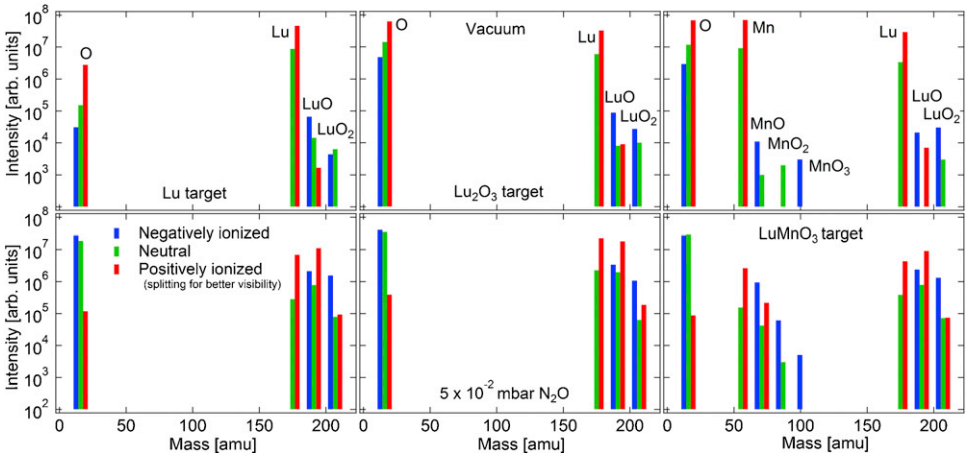


**Fig. 1.** Mass distributions for the three different targets (left to right: Lu, $Lu_2O_3$, $LuMnO_3$) under two different background gas conditions: the top row shows measurements in vacuum ($2 \times 10^{-1}$ mbar), the bottom row in $5 \times 10^{-2}$ mbar $N_2O$ gas.

triggered from the same photodiode placed in the beam path and used simultaneously to assure consistency of the results.

## 3. Results and discussion

### 3.1. Mass spectrometry

Mass spectrometry measurements performed on the three targets in vacuum and high $N_2O$ pressure ($5 \times 10^{-2}$ mbar) are shown in Fig. 1. All graphs are on the same logarithmic scale. Intensities for neutral species cannot be easily compared as the detection of neutral species is done via an ionization mechanism at the entrance of the mass spectrometer. For negative ionization, electrons of low kinetic energies are ejected from an iridium filament and then attach to the neutral plasma species. Changing to a high kinetic energy configuration leads to a process where the ejected electrons collide with the neutral species and strip them off their outer electrons leading to positive ionization. In both cases, different ionization cross-sections for different species and even the same species with different kinetic energies lead to unpredictable efficiencies < 1 and an unknown underestimation of intensities. Positively and negatively ionized species are detected with almost 100% efficiency and therefore a relative and absolute intensity comparison is possible. One interesting observation is the existence of neutral and ionized LuO species in vacuum when ablating from the Lu target. This indicates that the target is not pure Lu but contains small amounts of oxygen, resulting in a small LuO signal. A direct comparison to the $Lu_2O_5$ target shows that the contamination is minor as the oxygen signal in the latter is ~50 times higher than for the metallic target. Furthermore, the amount of ionized $LuO^+$ and $LuO^-$ detected for the Lu target is up to 8 times smaller than that detected for $Lu_2O_3$.

In $5 \times 10^{-2}$ mbar $N_2O$ all targets show a very similar behavior indicating that the target itself, e.g. its structure and/or actual composition, has only a very minor influence on the final composition of neutral and ionized Lu and LuO species in the plasma. Comparing the neutral and ionized Lu signals between vacuum and the $N_2O$ background a decrease of up to two orders of magnitude is observed for all targets. The importance of an oxidizing background can be seen when comparing the ratios of $LuO^+$ to $Lu^+$ in vacuum and background gas. For the Lu target it increase from 1:40,000 to 3:1, for the $Lu_2O_3$ target the increase goes from 1:3000 to 1:1 and in the case of $LuMnO_3$ the initial ratio is 1:2000 and the final one is 4:1. A similar observation is made for neutral LuO and Lu, as well as Mn and MnO species. Here only $MnO^-$ is observed with a ratio of 1:7000 compared to $Mn^+$. In the $N_2O$ background this ratio changes to 1:3. Overall, mass spectrometry clearly shows a decrease of the neutral and positively ionized metal species accompanied by an increase in the respective oxidized species indicating an oxidation process in the plasma in a $N_2O$ background.

### 3.2. Plasma imaging

While mass spectrometry gives information about composition and relative ratios of plasma species, it does not contain detailed information about the time and space resolved origin of oxidized species. To visually monitor this, a second measurement method has to be utilized. Plasma imaging offers the possibility to observe the plasma species behavior on the basis of emission lines of specific excited states of species and is therefore able to distinguish e.g. the metals and their oxides and how they behave during the ablation and expansion of the plasma plume.

In Fig. 2 the expanding plasma at different times after the laser impact is shown for an ablation from the Lu target. The top row shows the plasma with the AOTF set to 499 nm (Lu I) and the bottom row with a setting of 518.5 nm (LuO). The background changes from left to right from vacuum to $1.5 \times 10^{-3}$ and $5 \times 10^{-2}$ mbar $N_2O$. The intensity scales are kept constant with only the images from the highest pressure set to 1/10th of the intensity of the other gases. For these images the CCD was set to a gate width of 50 μs with a delay of 25 ns (minimum of the setup). For each Image 6 frames were accumulated to increase intensity and statistics. In total 409 images were taken with a 0.25 MHz spacing of the AOTF driver which corresponds to approx. 0.6 nm spectral change per image. Please note, the change in drive frequency for the AOTF is not linear with the transmission wavelength over the whole range. Two reflections are visible in the plasma images. On the left, near the impact region a reflection of the target holder surface can be observed and on the right the metallic surface of the mass spectrometer nozzle reflects the plasma light. As a result, the scaling of the pictures is known as the distance between target and mass spectrometer is set to 4 cm.

A clear trend is observed in Fig. 2, in vacuum the intensity of the Lu I line far surpasses the LuO line. Furthermore it extends roughly half way between target and mass spectrometer, corresponding to a distance of 2 cm. The LuO line shows intensity only directly after the laser pulse which can be related to a white light emission (Bremsstrahlung) in the very first nanoseconds of the plasma observable for the whole wavelength range. An increase of the background pressure results in increased intensities for both, the Lu I and LuO lines due to collisional re-excitation (center column